The Dispersion Inside Idealized Urban Street Canyons Under Atmospheric Stable Stratification

YanChing Q. Zhang
Lockheed Martin, U.S. EPA Scientific Visualization Center, P.O. Box 14365, 86 Alexander Drive
Research Triangle Park, North Carolina 27709, USA

Abstract: The effects of atmospheric stable stratification on the wind pattern and pollutant concentrations within two-dimensional urban street canyons are investigated using a k-epsilon turbulence model TEMPEST. The influences of two incident stable stratified sheared turbulent inflows are calculated and compared. The numerical simulation results demonstrate significant influences on the wind structure and pollutant concentrations within the street canyons due to different building configurations as well as incident stably stratified boundary conditions. In particular, changes in the recirculating flow pattern above the street and on top of the canyon buildings affects the pollutant transport within and out of the street canyon. The influences are much weaker after the second or third downstream street canyon.

1. INTRODUCTION

The term street canyon refers to a relatively narrow street between a row of buildings. The street canyon is the basic geometric unit comprising the urban canopy. Air flow within the urban boundary layer is dominated by microscale influences. Most studies on pollutant dispersion in an urban area using numerical methods have been primarily site specific. In Zhang and Huber (1995), the effects of neutral stratification on the flow and dispersion inside a group of idealized street canyons were investigated. This paper is a continued effort of the study.

In this paper, we apply the same numerical model (the TEMPEST) to investigate dispersion inside the same group of idealized (two-dimensional) urban street canyons with upstream flow normal to the canyon. Five two-dimensional cases were studied and compared to investigate the effects stable stratification on concentration levels in the vicinity of the street canyon with five canyon configurations. The results provide some insight into the generalized flow structure as well as the dispersion patterns under stably stratified boundary condition with different geometric configurations. Only emissions from a ground source are examined herein. The effects of the canyon geometric configurations and number of the canyons in the wind direction under stable stratification on the concentration field are discussed.

2. NUMERICAL SIMULATION

2.1. Introduction to the TEMPEST Model:

The TEMPEST (Transient Energy Momentum and Pressure Equations Solution in Three-dimensions) model is a three-dimensional, time-dependent, nonhydrostatic numerical model that was developed at Battelle Pacific Northwest Laboratory; it has been applied to a broad range of engineering and geophysical problems (Trent and Eyler, 1989). The TEMPEST model includes the ability to account for small density variations through the Boussinesq approximation. Cylindrical, Cartesian, or polar coordinates may be used. It has the ability to use variable grid spacing along any coordinate, and the inflow/outflow boundaries can be either specified or computed. Turbulence is treated by using a turbulent kinetic energy/dissipation (k-ε) model. The solution technique in TEMPEST is similar to the SMAC (Simplified Marker-And-Cell) technique (Amsden and Harlow, 1970), whereby at each time step, the momentum equations are solved explicitly and pressure equations implicitly; temperature, turbulent kinetic energy (TKE), dissipation of kinetic energy (DKE), and other scaler transport equations are solved by using an implicit continuation procedure. The standard formulation for the k-ε turbulence model (Trent and Eyler, 1989) is used in our simulation, and a staggered grid system is adopted.

The governing equations for the k-ε model (as used in TEMPEST) in a Cartesian coordinate system are presented below. We neglect molecular diffusion in comparison with turbulent diffusion in the momentum equations, and confine our simulations to the atmospheric surface layer over a small domain (say, 5km×5km), so that Coriolis effects can also be neglected. The governing equations, subject to Boussinesq approximations and Reynolds averaging, are:

Continuity:

$$\frac{\partial U_i}{\partial x_i} = 0 \qquad (1)$$

Momentum:

$$\frac{\partial U_i}{\partial t} + U_j \frac{\partial U_i}{\partial x_j} = -\frac{\partial}{\partial x_i}\left[\frac{\delta P}{\rho_0} + \frac{2}{3}k\right] + \frac{\partial}{\partial x_j}\left\{\nu_t\left[\frac{\partial U_i}{\partial x_j} + \frac{\partial U_j}{\partial x_i}\right]\right\} - \frac{\delta \rho}{\rho_0} g \delta_{3i} \qquad (2)$$

State:

$$\frac{\delta \rho}{\rho_0} = -\frac{\delta T}{T_0} \tag{3}$$

Thermal energy:

$$c_p \frac{\partial T}{\partial t} + c_p U_j \frac{\partial T}{\partial x_j} = \frac{\partial}{\partial x_j}\left[\frac{\nu_t}{Pr_T}\frac{\partial T}{\partial x_j}\right] + Q \tag{4}$$

Concentration equations:

$$\frac{\partial C^i}{\partial t} + U_j \frac{\partial C^i}{\partial x_j} = \frac{\partial}{\partial x_j}\left[D_j \frac{\partial C^i}{\partial x_j}\right] + S^i \tag{5}$$

where U_i is the ith mean velocity component, t is time, $\delta\rho$ is the deviation of density from its reference value ρ_0, δP is the deviation of pressure from its reference value, ν_t is an effective viscosity which is the sum of molecular viscosity (which is neglected in our simulations) and turbulent eddy viscosity, g_i is the ith component of acceleration due to gravity, c_p is the specific heat of air at constant pressure; Pr_T is the turbulent Prandtl number, Q is the volumetric heat generation rate, C_i is the mean mass fraction of the ith constituent, D_j is the effective mass diffusivity in the jth direction (which is the sum of turbulent and molecular mass diffusivities), S_i is the mass generation rate, and k is the turbulent kinetic energy (TKE), which is defined as:

$$k = \frac{1}{2}\left[\overline{(u)^2} + \overline{(v)^2} + \overline{(w)^2}\right] \tag{6}$$

where u, v and w are the velocity fluctuations in the x, y and z directions, respectively. The above equations treat density as a constant (incompressible flow) except in the body force term of the momentum equation, which allows us to simulate the stratification. The Reynolds stresses and fluxes have sometime been modeled or parameterized using the gradient transport relations to close the above system of equations. TEMPEST uses a k-ϵ turbulence model to close the above system of equations by providing estimates of effective turbulent viscosity and mass diffusivity. This is accomplished by using transport equations for the turbulent kinetic energy k:

$$\frac{\partial k}{\partial t} + \frac{\partial k U_j}{\partial x_j} = \frac{\partial}{\partial x_j}\left[\frac{\nu_t}{\sigma_k}\frac{\partial k}{\partial x_j}\right] + (S+G) - \epsilon \tag{7}$$

and the dissipation of turbulent kinetic energy,

$$\frac{\partial \epsilon}{\partial t} + \frac{\partial \epsilon U_j}{\partial x_j} = \frac{\partial}{\partial x_j}\left[\frac{\nu_t}{\sigma_\epsilon}\frac{\partial \epsilon}{\partial x_j}\right] + \frac{\epsilon}{k}(C_1 S + C_3 G) - C_2\frac{\epsilon^2}{k} \tag{8}$$

where ν_t is the kinematic (molecular) viscosity:

$$\epsilon = \nu_t^2 \overline{\left(\frac{\partial u_i}{\partial x_j}\right)^2} \tag{9}$$

Here S is the shear production term, G is the buoyancy term in the TKE equation (7), defined as:

$$S = \nu_t\left[\frac{\partial U_i}{\partial x_j} + \frac{\partial U_j}{\partial x_i}\right]\frac{\partial U_i}{\partial x_j} \tag{10}$$

$$G = \frac{\nu_t}{\sigma_t}\frac{g}{\rho_0}\frac{\partial \rho}{\partial z}\delta_{3i} \tag{11}$$

where σ_t, σ_ϵ and σ_k are three of the empirical constants in k-ϵ models. The effective diffusivity of momentum is estimated as $\nu_t = C_\nu k^2/\epsilon$. The effective diffusivity of mass is $D = \nu_t/Sc_T$, where Sc_T is the turbulent Schmidt number. The standard values of constants which have been used for most engineering applications (Gibson and Launder, 1978; Zhang et al., 1993) used in the TEMPEST are:

$(\sigma_t, \sigma_k, \sigma_\epsilon, C_1, C_2, C_3, C_\nu, Sc_T, Pr_T) = (0.9, 1.0, 1.3, 1.44, 1.92, 1.44, 0.09, 0.77, 0.9)$.

2.2. Boundary Conditions:

Two sets of stable stratified approaching flow were applied to 10 numerical simulations. The simulations with the lightly stable stratified approach flow are designated as case L; those with the extreme (more) stable stratified approach flow are designated as case M.

In both cases L and M, $\rho c_p(u_*\theta_*) \approx 40 w/m\cdot s$ or $u_*\theta_* = 0.03333 m\cdot K/s$ is applied, where $\rho = 1.212 kg/m^3$ is the density of the air at 111m; $c_p = 1004.67 m^2/s^2K$ is the specific heat of air. In case L, we have $u_* = 0.29 m/s$ and $\theta_* = 0.11K$; In case M, we have $u_* = 0.11 m/s$ and $\theta_* = 0.29K$.

In both cases, the logarithm distributed approaching flow and temperature fields are used (Lacser and Arya, 1986), assuming $z_0 = 0.1$ m:

$$U = \frac{u_*}{\kappa}\left[\ln\left(\frac{z}{z_0}\right) + 5\frac{z}{L}\right] \tag{12}$$

$$\theta - \theta_0 = \frac{\theta_*}{\kappa}\left[\ln\left(\frac{z}{z_0}\right) + 5\frac{z}{L}\right] \tag{13}$$

where κ is the von-Karman constant, i.e., $\kappa = 0.4$; θ_0 is the reference potential temperature, i.e., $\theta_0 = 293K$ (20°C); L is the Obukhov length which is defined as: $L = \theta_0 u_*^2/\kappa g\theta_0$, and g is the gravity acceleration velocity. The boundary layer height h is obtained from: $h = 0.4(u_*L/f)^{1/2}$ (Businger and Arya, 1974), where

$f \approx 10^{-4} s^{-1}$ is the Coriolis parameter.

In other words, in case L, the Oblukhov length L≈57m, which represents the upstream approaching flow is slightly stable, and the corresponding mixing layer height h≈162m. In case M, the Oblukhov length L≈3.1m, which represents the upstream approaching flow is slightly stable, and the corresponding mixing layer height h≈23m.

The turbulent kinetic energy (TKE) in the approach flow used the relationship from Lacser and Arya (1986):

$$k = 4.92\ (1 - \frac{z}{h})^{1.32} u_*^2 \qquad (14)$$

The boundary conditions for dissipation of TKE ε are resolved by using the formula at the steady state from Brost and Wynggard (1978):

$$\varepsilon = [\frac{u_*^3}{\kappa h}](\frac{h}{z})\,[1+3.7(\frac{z}{h})(\frac{h}{L})]\,(1-0.85\frac{z}{h})^{1.5} \qquad (15)$$

2.3 Simulation Configuration and Model Set-Up:

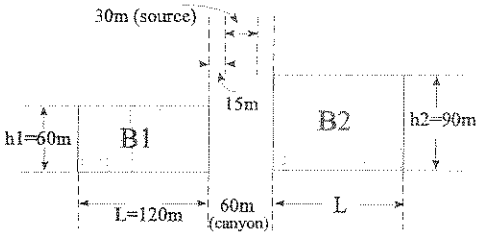

Figure 1: The side view of the generalized 2-D buildings and the street canyons for numerical simulations.

The buildings were arranged to provide cases having 1, 2, or 4 street canyons. The influences of the two-dimensional building heights are examined by using combinations of a 60m building height (B1) and a 90m building height (B2). In all cases, the building width is constant at 120 m and the urban street canyon (SC) width is 60 m. The pollutant source is located at the center of the street with a width of half of the street canyon (i.e., L_{source}=30m) (Figure 1).

A variable-spaced grid of 37 cells in the vertical direction is used in all simulations; and the variable-spaced grid in the longitudinal direction depends on the length of the domain, it varies from 86 cells (for one canyon) to 170 (for four canyons). The smallest cell dimension (3 m) in the domain is one twentieth of the building height.

case L (lightly stable)	case M (more stable)	Canyon Configuration
L1	M1	B1-SC-B1
L2	M2	B1-SC-B2
L3	M3	B2-SC-B1
L4	M4	B2-SC-B1-SC-B2
L5	M5	B2-SC-B1-SC-B2-SC-B1-SC-B2

Table 1: Geometric configuration and upstream boundary conditions for numerical simulations (SC = Street Canyon).

The computed fields of U_i, k, and ε from TEMPEST, as discussed above, are used to calculate the concentration field for the street level sources under five different street canyon types in each case group (see Table 1). The concentration field was calculated by solving concentration transport equation (Zhang et al., 1993) with the first-order closure scheme.

Considering the computing time and machine memory requirements, these idealized two-dimensional street canyon simulations are possible on either a personal computer or a workstation.

3. RESULTS AND DISCUSSIONS

3.1 The Influences of the Canyon Configurations:

3.1.1 *Single Canyon:*

Five simulations with two different building type (B1 & B2) combinations were conducted to investigate the influence of geometric configurations on the dispersion inside the idealized urban street canyons under stable stratified approach flow. We found that our current findings support our conclusions in our previous paper (Zhang and Huber, 1995).

Only cases M1, M2, and M3 (consisting of one canyon) and M5 (four canyons) are presented here. Figures 2, 3, and 4 display the concentration contour fields around a two-dimensional street canyon. All of the one-canyon cases (M1, M2, and M3) have a very similar flow pattern before the upstream edge of the upwind building. The flow structure before the upstream building had negligible effects on the overall dispersion fields. A recirculation zone exists on the top of the upstream building in all three cases. In both cases M1 and M2 (Fig. 2, Fig. 3), the flow just above the first building recirculation zone passes smoothly downstream, tending to remain at the same level above the ground. In case M3 (Fig. 4), flow above the recirculating zone remains at the same vertical level above the vortex on the top of the upstream building as it passes over a recirculation region over the downstream building. The reversed flow on top of the upstream building draws the pollutants from the canyon to the roof of the upstream building in all three cases.

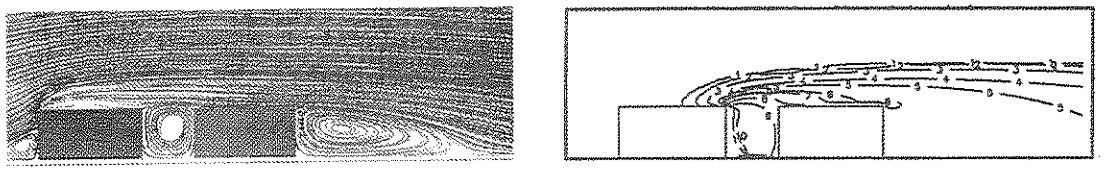

Figure 2: Dispersion fields around street canyon in case M1. (a) streamlines; (b) Contours of the constant concentrations. The concentration levels are (g/m^2):

1 — 10^{-4}	2 — 10^{-3}	3 — 10^{-2}	4 — 10^{-1}
5 — 0.2	6 — 0.4	7 — 0.5	8 — 1.0
9 — 2.0	10 — 4.0	11 — 5.0	

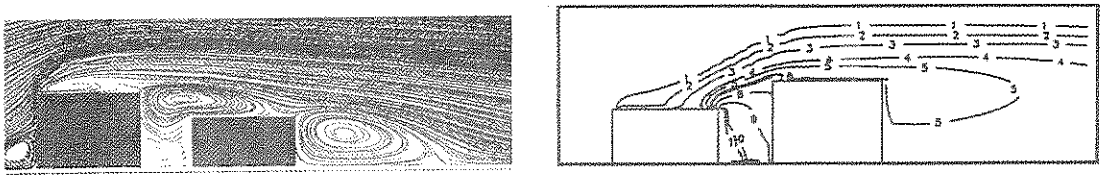

Figure 3: Dispersion fields around street canyon in case M2. The contour levels are the same as in Figure 2.

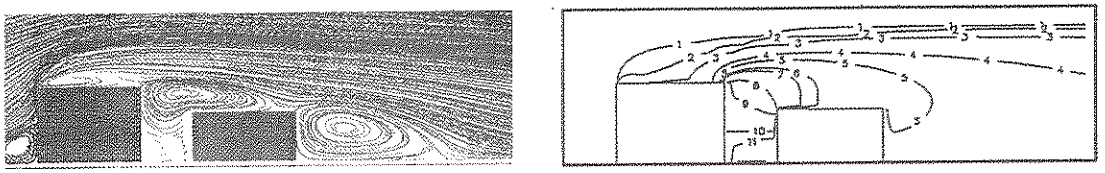

Figure 4: Dispersion fields around street canyon in case M3. The contour levels are the same as in Figure 2.

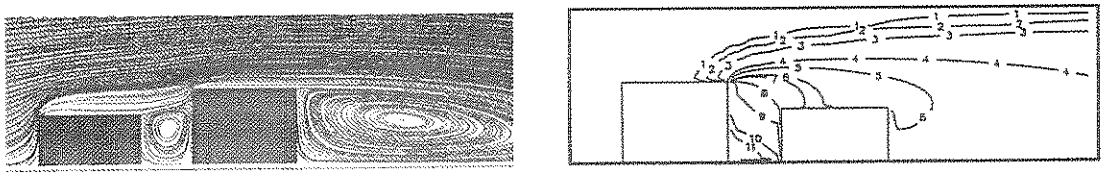

Figure 5: Dispersion fields around street canyon in case L3. The contour levels are the same as in Figure 2.

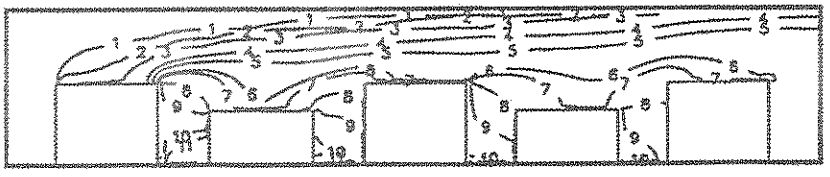

Figure 6: Dispersion fields around street canyon in case M5. The contour levels are the same as in Figure 2.

In case M1, with the buildings on both sides at an equal height, there was one single large vortex generated in the gap between the buildings. The size of this vortex is about the size of this gap. In case M2, with the downwind building 1.5 times as tall as the one upwind, the flow passing over the first building is somewhat blocked by the second one. Again a single vortex is formed in the canyon. The size and shape of the vortices inside the canyon for M1 and M2 depend on the relative height of the buildings at both sides of the canyon. In case M3, the upwind building is 1.5 times higher than the downwind one, and the flow goes downward as it passes. This downward flow had a tendency to form a big wake behind the upstream building. Since there is a second building in this potential wake, the flow hits the second building roof and goes back upstream, forming two counter-direction recirculating vortices: The clockwise one that is larger and stronger overlaps the step-down building, and the canyon itself generates a secondary counter-clockwise vortex at the bottom of the canyon.

The differences in canyon configurations result in different dispersion patterns, and the maximum concentration shifts from the downstream side of the canyon in U3 to the upstream side of the canyon in M1 and M2 (Fig. 2 and Fig. 3). The concentration on the upstream side of the canyon is twice as high as that on the downstream of the canyon in case M1 and M2, whereas the concentration downstream of the canyon is several times as high as that on the upstream side of the canyon in M3 (Fig. 4).

In cases M1 and M2, both the height and length of the wake behind the downstream building depend mainly on the downstream building height. In case U3, the strong reversed flow above the second building elevates the flow above the canyon, and it tends to increase the height of the wake. However, the resulting wake length behind this building is smaller than that in case M1 due to the strong stably stratified upstream flow. We will discuss the phenomena in the next section.

3.1.2 *Multiple Canyons:*

In urban atmospheric environments, most situations have several canyons in a row. So, we extended our simulations to include cases involving two and four canyons.

When two or more street canyons are involved (cases M4 and M5), we found that the flow and dispersion patterns in the first canyon simply depend on the upstream conditions and the relative heights of the buildings beside the canyon; those inside the following canyons have flow and similar dispersion patterns. Figure 6 presents case M5 with four canyons in the downwind direction. The concentration contour pattern inside the first canyon is very similar to that in case M3; that inside the second canyon is similar to that in the second canyon in the L2 (Figure 5), which has the lightly stable stratified inflow, but has dramatic differences from that in case M2. The contour pattern inside the fourth canyon still has some of the characteristics of L4. Our results show that the dispersion fields have steady structure after two canyons.

3.2 Effects of Stable Stratifications:

As a demonstration of the effects of different stable stratification, the results from only one pair of simulations (L3 and M3) are presented (Figures 4 and 5).

The effects of stable stratification is strongly felt on the mean and turbulence fields when the approach flow becomes extremely stable (case M). Similar as discussed in Zhang et al (1995), when the approach flow is only slightly stable (case L), the flow fields behave more like a fully developed turbulent flow, and hence turbulence plays an important part in the diffusion process (Figure 5). In other words, the enhanced turbulence mixing and thickening of the shear layers shed from the windward edges of the building apparently promote flow reattachment on the building surfaces. There are several orders of magnitude difference about the concentration on the roof of the first building between the two groups (L and M). Pollutants emitted within a canyon will generally not be transported to the front of the upstream buildings. The recirculating flow above the upstream building depends more strongly on the upstream boundary conditional than the relative canyon configuration.

The flow pattern changes dramatically inside the canyon. Flow is stronger because of the extreme stably stratified appearance upstream flow. The stronger vortex on the top of the canyon transfers the pollutants downstream of the canyon, the concentration on the top of the second building in case M3 is higher than that of case L3.

We should mention here, the recirculating wake size inside and above the canyon is much smaller that those with the same canyon configuration, but in the neutrally stratified approach flow (Zhang and Huber, 1995). However, the flow passing the first building still reattaches further away from the canyon, the reattachment point is at the downstream building top, and the resulting reversed flow is stronger, which produces a secondary recirculation circle at the bottom of the canyon in case M3. In case L3, the flow falls downward as it passes the first block. This downward flow reattaches inside the canyon. The flow does not even reach the second building roof like that in M3, which has an opportunity to form two counter direction recirculating vortices.

Zhang et al (1993) showed that for a neutral approach flow, the less the upstream turbulence, the larger is the cavity size behind the building. The ambient turbulence tends to induce reattachment on the roof., which in turn reduces the size of the cavity size behind the building. In case L, the turbulence in the upstream is stronger than that in case M, all the recirculations on the top of the upstream building disappear in case L. In case M, the strong stably stratified environment tend to promote the strong downflow behind the second building. The wake size behind the second building is smaller that in group L.

Similar effects of the upstream stable stratification on the dispersion around street canyons are found in other cases.

4. CONCLUSIONS

Our study was limited to the cases investigated. A different ratio of building height to street canyon width will influence dispersion patterns in the vicinity of the canyons. This is one of the continuous effects on the subject. Our results in this paper are consistent with the conclusions we reached in our previous paper.

The stable stratification combined with canyon geometric configuration have significant influences on the concentration fields in the vicinity of urban street canyons.

Pollutants emitted within a canyon will generally not be transported to the front of the upstream buildings. The recirculating flow above the upstream building depends more strongly on the upstream boundary conditions than the relative canyon configuration. The flow and concentration pattern inside the canyon depend on both the upstream flow conditions (stable stratification) and the relative heights of the buildings on both sides of the canyon. The dispersion fields behind the downstream building depend on both the flow characteristics within the canyon and the downstream building height. The strong stable stratification has large effects on the flow and dispersion structure in the vicinity of the canyons, it tends to decrease the turbulence mixing inside the recirculating zones. The vertical and horizontal diffusion is weakened by the stratification, especially inside the wakes. The mean flow tends to be stronger.

The high concentration stays on the upstream side of the building, except in the step-down canyon cases M3, M4, and M5, which have the extremely stable stratified inflow.

When there is more than one canyon in the downwind direction, the upstream stably stratified flow conditions can be very critical to the dispersion fields inside the first canyon, but they are not as important to the concentration fields inside the consecutive canyons. The dispersion fields in the vicinity of the first canyon are very similar to the corresponding cases involving only one canyon and the same upstream boundary conditions. The fields in the vicinity of the following canyons appear to depend more on the relative geometric configuration on two sides of the canyon than the degree of the stable stratification in the upstream. In other words, the strong stable stratification in the upstream flow has minimal effects on the dispersion beyond the first canyon.

5. DISCLAIMER

This work has been funded in part by the U.S. Environmental Protection Agency under contract 68-D0-0106 to ManTech Environmental Technology, Inc. Mention of trade names or commercial products does not constitute endorsement or recommendation for use. The author is grateful for the help and advice of Dr. Alan Huber in connection with the project.

6. REFERENCES

Amsden A.A. and Harlow F.H. (1970): The SMAC Method: A Numerical Technique for Calculating Incompressible Flows, Report LA-4370, Los Alamos Scientific Laboratory, Los Alamos, NM, 85p.

Arya S.P. (1988): *Introduction to Micrometeorology*, International Geophysical Series, Ed. R. Dmowska and J.R. Holton, Academic Press, Inc., 303pp.

Brost R.A. and J.C. Wynggard (1978): A Model Study of the Stably Stratified Planetary Boundary Layer, *J. Atmos. Sci.*, 35, 1427-40.

Businger J.A. and S.P. Arya (1974):Height of the Mixed Layer in a Stably Stratified Planetary Boundary Layer, *Advances in Geophysics*, 18A, Academic Press, 428pp.

Lacser A. and S.P. Arya (1986): A Numerical Model Study of the Structure and Similarity Scaling of the Nocturnal Boundary Layer, *Boundary-Layer Meteorology*, 35, 369-385.

Trent S.D. and Eyler L.L. (1989): TEMPEST, A Three-Dimensional Time-Dependent Computer Program for Hydrothermal Analysis, Volume 1: Numerical Methods and Input Instructions, PNL-4348, Pacific Nothwest Laboratory, Battelle, WA.

Zhang Y.Q., Huber A.H., Arya S.P. and Snyder W.H. (1993): Simulation to Determine the Effects of Incident Wind Shear and Turbulence Level on the Flow Around a Building, *J. Wind Engr. Indus. Aerodyn.*, 46&47, 129-134.

Zhang Y.Q., Arya S.P. and Snyder W.H. (1995): A Comparison of Numerical and Physical Modeling of Stable Atmospheric Flow and Dispersion Around a Cubical Building, accepted by *Atmospheric Environment*.

Zhang Y.Q. and Huber A.H. (1995): The Influence of Upstream Wind Shear and Turbulence on the Wind Pattern and Pollutant Concentrations Within Street Canyons: A Numerical Simulation Study, *Reprints of 11th Symposium on Boundary Layer and Turbulence*, Charlotte, NC, 196-199.